J Porous Mater (2013) 20:331–338
DOI 10.1007/s10934-012-9602-1

Investigation of structural properties of clinoptilolite rich zeolites in simulated digestion conditions and their cytotoxicity against Caco-2 cells in vitro

Dilek Demirbüker Kavak · Semra Ülkü

Published online: 4 June 2012

Abstract The use of the clinoptilolite rich natural zeolites in biomedical applications such as in anticancer therapy, drug or drug support systems and as nutritive supplement is highly dependent on their behavior in digestive conditions. Aim of this study is to investigate structural stability of clinoptilolite rich natural zeolites in simulated digestion conditions and their interactions with digestive media and with Caco-2 (human colon adenocarcinoma) cells. X-ray Diffraction (XRD), Fourier Transform InfraRed (FTIR), Scanning Electron Microscopy (SEM) and Inductively Coupled Plasma Atomic Emission Spectroscopy (ICP-AES) analyses of the clinoptilolite rich zeolite samples showed that zeolites preserved their structural stabilities during in vitro digestion. Slight interactions were detected in UV measurements of the digestive liquid media and FTIR spectra of the intestinal digested media powders. SEM results implied that zeolites might have a role in the aggregation of the digestive enzymes. Cytotoxicity test using colon cancer cells showed that clinoptilolite rich natural zeolites have cytotoxic effect against Caco-2 cells and cytotoxicity did not significantly change with respect to simulated digestion process.

Keywords Zeolite · Clinoptilolite · Simulated digestion · Caco-2 · Cancer cell

D. D. Kavak (✉)
Food Engineering Department, Engineering Faculty, Afyon Kocatepe University, ANS Campus, 03200 Afyonkarahisar, Turkey
e-mail: dkavak@aku.edu.tr

S. Ülkü
Chemical Engineering Department, Engineering Faculty, Izmir Institute of Technology, Gulbahce Koyu, 35430 Urla Izmir, Turkey

1 Introduction

Natural zeolites are porous, crystalline, hydrated alumina silicates of alkaline or alkaline earth metals. Their framework consists of SiO_4 and AlO_4 tetrahedra linked through common oxygen atoms. They act as molecular sieves, have adsorptive, ion exchange, catalytic properties and their high stability and low cost make them useful in numerous industrial, agricultural, chemical and environmental applications [1–3].

In recent years, one of the exciting potential applications of natural zeolites is in medical area. Natural zeolite clinoptilolite has been reported to be nutritionally inert adsorbent and non-toxic to animals [4, 5] which make clinoptilolite very advantageous. Several studies demonstrated that clinoptilolite supplementation was well tolerated by animals such as it resulted significant feed conversion and promoted biomass production, weight gain and animal health [6–11]. Clinoptilolite was used to protect animals from feed-originated toxins by adsorbing toxic compounds in gastrointestinal tract and by preventing their passage to circulatory system [12–14]. Also, it was reported to decrease the deposition of radioactive compounds in animals administered to the contaminated feed and it reduced oxidative stress in animals after partial hepatectomy [15, 16]. Purified natural clinoptilolite was reported to be harmless to the human body [17] and was used as antidiarrheaic drug [18] and as antiacid agent for humans suffering from the hyperacidity without showing any toxic or biological hazard [19, 20]. A novel use of micronized clinoptilolite as a potential adjuvant in anticancer therapy was reported [21]. It was used in anticancer treatment of mice and dogs suffering from cancer and it resulted prolonged of life span and improvement of health status.

It is clear that biological effect of natural zeolite will depend on its behavior in physiological systems where

digestive system has prior importance. Available data primarily focus on using zeolites as drugs or drug supports [18, 19, 22]. However, investigations of natural zeolite's behavior only in simple buffer solutions or in batch experiments for medical purposes will be insufficient to reflect the complicated digestion media where there were also digestive enzymes or bile salts.

Aim of the present study is to investigate the structural stability of clinoptilolite rich natural zeolites in complex simulated digestion conditions and their possible interactions with digestive media considering the gastric and intestinal digestion as a continuous process. Additionally, cytotoxic effects of zeolite's digested and nondigested forms against colon cancer cells (Caco-2) were investigated in vitro. Regarding the novel uses of zeolites in biochemical applications, this study will be focused on the behavior of clinoptilolite rich zeolites in complicated simulated digestion conditions for their further uses as drugs/drug release matrices and in cancer therapies. In this study, special interest has been devoted to clinoptilolite-rich natural zeolite because of the abundance of the raw material in our country. 50 billion tons of raw material reserve having high mineral purity and homogeneity in Gördes basin (Western Anatolia) was estimated [23].

2 Materials and methods

2.1 Materials

Clinoptilolite rich mineral specimens were obtained from Gördes region of Western Anatolia. The mineral was mainly made up of clinoptilolite (80–85 %) and additionally, quartz (5–10 %), and analcime + mordenite (<5 %) [24]. It was ground and sieved at 45–75 μm size. Porcine bile extract, pepsin and pancreatin, NaOH, $NaHCO_3$, HCl used in digestion experiments were purchased from Sigma (Germany). In cell culture studies Caco-2 (Human, colon adenocarcinoma cell line) cells were purchased from Şap Institute (Turkey). Dulbecco's Modified Eagles Medium (DMEM), fetal bovine serum (FBS), PBS buffer, tyripsin, L-glutamine and penicillin/streptomycin antibiotics were purchased from Biological Industries (Israel). MTT (3-(4,5-dimethylthiazolyl-2)-2,5-diphenyl tetrazolium bromide) solution and dimethyl sulfoxide (DMSO) were purchased from Sigma (Germany).

2.2 Simulated digestion and characterization experiments

Simulated digestion experiments were performed by the modification of the procedure reported by Ferruzzi et al. [25]. Gastric fluid was prepared with 0.1 M HCl and 3.2 mg ml^{-1} pepsin. pH adjustment was made using 0.1 N NaOH where final pH of gastric fluid was 2.0. Digestion experiments were performed with zeolite against control experiments (without zeolite). Final zeolite concentrations in simulated digestion conditions were 3 g $(100\ ml)^{-1}$. Gastric fluids were incubated at 37 °C in a water bath shaking at 95 rpm for 1 h. Samples obtained after this step were named as gastric digested samples coded with "G" throughout the text. Then, the pH of the gastric digested fluid was raised to 5.5 by adding 1 M $NaHCO_3$ followed by the addition of a mixture of bile extract and pancreatin (including amylase, lipase and protease) prepared in 0.1 M $NaHCO_3$. Final concentrations for the bile extract and pancreatin were 2.4 and 0.4 mg ml^{-1}, respectively. The pH of each sample was increased to 7.5 by the addition of 1 N NaOH. Samples were incubated at 95 rpm at 37 °C for 2 h to complete the intestinal phase of the in vitro digestion process. Samples obtained after this step were called as digested samples and coded with "D" throughout the text. Simulated gastric and intestinal digestion media were analyzed for their UV absorption properties. 100 μl of each sample obtained immediately after gastric and intestinal digestion steps were put in 96-well plates. Samples were analyzed in triplicate for their UV absorption spectra in the range of 200–380 nm by microplate reader (Varioskan, Thermo).

After simulated digestion procedure, solid (zeolite) and liquid phases of the gastric and intestinal digested media were separated by centrifugation (Rotofix 32, Hettich, UK) at 800 g for 5 min. Both zeolite and liquid phases were frozen at −18 °C for 2 h and freeze dried for 24 h by lyophilizator (Telstar Cryoduos Lyobeta 50, Spain). Then they were kept +4 °C until the day of analyzes. Mineralogy and the crystallinity of the zeolite samples were determined by powder X-ray diffraction techniques (Philips X-Pert Pro) using CuKα radiation in the range of 2θ: 2°−40° with 0.2° step size. Elementary composition of control (untreated) and digested zeolite samples were determined by ICP-AES (96, Varian). Solid (zeolite) phases and lyophilized liquid phase powders were analyzed by scanning electron microscopy (SEM) to view the surface morphology. Photographs were taken at an accelerating voltage of 15 kV, depending upon the sample at different magnifications in a Phillips XL30S FEG electron microscope. IR characterizations were carried out between 400 and 4,000 cm^{-1} by Shimadzu FTIR-8201 model Fourier Transform Infrared Spectrometer.

2.3 Cell culture experiments

Caco-2 cells (human colon adenocarcinoma cells) were cultured in DMEM supplemented with 10 % FBS, 1 % L-glutamine, 1 % nonessential amino acids, and 50 μg/ml

penicillin–streptomycin. The cell cultures were maintained at 37 °C in a 95 % humidified atmosphere with 5 % CO_2 where they were seeded onto collagen-coated 25 cm^2 area culture flasks. Caco-2 cells were fed twice weekly and were subcultured (passaged) with 0.25 % trypsin and 0.2 % EDTA (5–10 min) at 37 °C and seeded in new flasks for every 10–14 days.

For the zeolite treatments, cells were harvested by trypsinization after 80 % confluency was reached. They were seeded at a density of 10^5 cells/cm^2 in 96-well plates (Becton–Dickinson, Meylan, France). Zeolite samples were sterilized and added in culture media so that the final zeolite concentrations were 25, 50 and 75 mg/ml. They incubated with cell culture media for 24 h at 37 °C. After incubation treated media was distributed into wells in triplicate where Caco-2 cells were seeded. Positive and negative controls were prepared and incubated in the same manner as the experimental specimens. After 24, 48 and 72 h incubation, MTT cell proliferation assay was performed.

2.4 MTT cell proliferation assay

Caco-2 cell viability was measured by MTT cell proliferation assay. The yellow tetrazolium salt; MTT (3-(4,5-dimethylthiazolyl-2)-2,5-diphenyltetrazolium bromide) was reduced by metabolically active cells, in part by the action of dehydrogenase enzymes, to generate reducing equivalents such as NADH and NADPH. The resulting intracellular purple formazan was solubilized and quantified by spectrophotometric means. 20 µl MTT solution was added to each well and shaken to thoroughly mix the MTT into the media. Cells were incubated under 95 % humidified air and 5 % CO_2 atmosphere at 37 °C for 4 h to allow the MTT to be metabolized in accordance with the manufacturer's instructions. Cell media was dumped and formazan dye was resuspended in dimethyl sulfoxide (DMSO) and well was shaken to thoroughly mix the formazan into the solvent. Optical density was measured at 540 nm by Multiskan Spectrum (Thermo) which was directly correlated with cell quantity.

3 Results and discussion

3.1 Changes in UV absorption spectra of liquid phase in simulated digestion studies

UV spectra of the digestive media incubated with zeolite were analyzed to investigate the possible interactions between protein structures and zeolites such as adsorption. Digestive media without zeolite incubation was used as control. Changes in the maxima of the UV absorption spectra of liquid digestion media might indicate the changes in the amount of enzyme levels. Results of the UV spectra of liquid digestion are given in Fig. 1. UV absorbance at around 270 nm corresponds to the digestive enzymes in protein structure. Results in Fig. 1 for digestion fluids (D and DZ) indicate that there is not a considerable interaction with zeolite and digestion fluid which was consisted of amylase lipase and protease. This is also important for the digestive role of enzymes. For gastric media including pepsin enzyme (G), slight fluctuations in absorbance values were observed with zeolite incubation. Those interactions might be related to the continuous changes of the pH and ionic strength of the simulated digestion media. Thus, active sites on the zeolite and protein surfaces might be affected. The active sites on zeolite surface are Si–OH and Al–OH groups. In acidic to neutral pH range, protonation of negative and neutral surface hydroxyl groups were reported [26]:

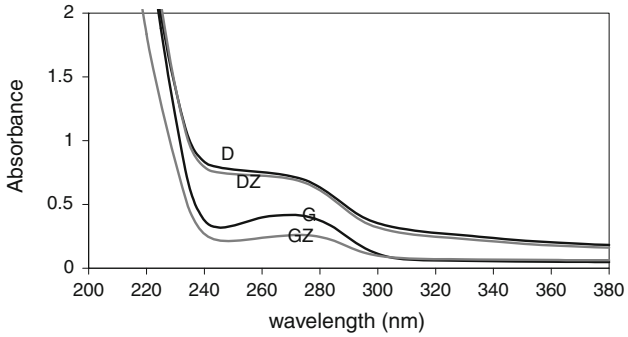

Fig. 1 UV spectra of gastric and digestion fluids (*G* control gastric fluid, *GZ* gastric fluid incubated with zeolite, *D* control digestion fluid, *DZ* digestion fluid incubated with zeolite

$$\equiv \mathrm{Al} - \mathrm{OH} + \mathrm{H}^{+}_{\mathrm{aq}} \Leftrightarrow \equiv \mathrm{Al} - \mathrm{OH}^{+}_{2} \quad (1)$$

$$\equiv \mathrm{Si} - \mathrm{O}^{-} + \mathrm{H}^{+}_{\mathrm{aq}} \Leftrightarrow \equiv \mathrm{Si} - \mathrm{OH}. \quad (2)$$

On the other hand, pepsin has only two basic groups and 20 carboxyl groups and at pH higher than 1 (pI), it has a negative electrical charge [27]. Therefore, electrostatic interactions between the COO− groups and Al–OH_2^+ groups might be active and might result reduction of the spectral maxima which corresponds to reduction of free enzyme level in liquid media. Beside the electrostatic interactions, there could be hydrogen bonding between hydroxyl (−OH) groups on the zeolite and H-bond acceptors on the enzyme depending on the chemical nature of the protein chains and zeolite. It was important to note that zeolite has also small amounts of impurities such as quartz. Quartz might be responsible for the interaction of pepsin enzyme where it was also reported to be used in protein adsorption [28].

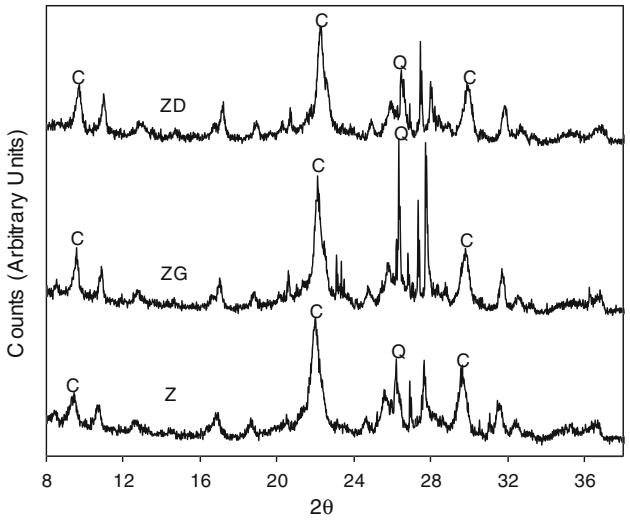

Fig. 2 XRD patterns of zeolites; *Z* control-untreated zeolite, *ZG* gastric treated zeolite, *ZD* digested zeolite (*C* clinoptilolite peaks at $2\theta = 9.81°$, 22.3° and 30°; *Q* quartz peak at $2\theta = 26.62°$)

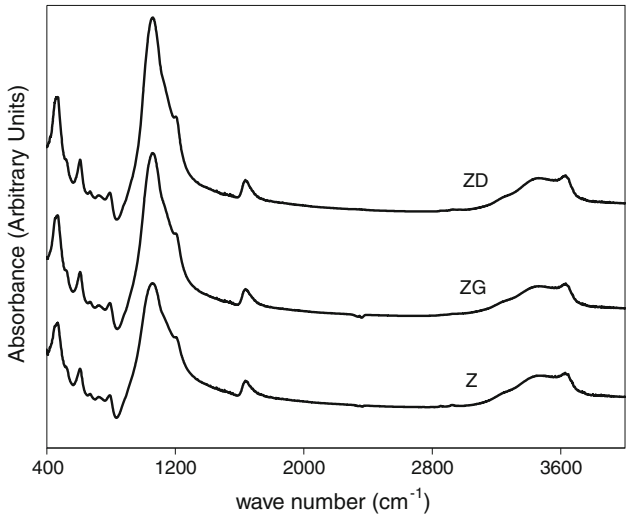

Fig. 3 Infrared spectra of zeolite samples (*Z* control-untreated zeolite, *ZG* gastric treated zeolite, *ZD* digested zeolite)

3.2 Characterization results

XRD results for the digested and non-digested zeolite samples are given in Fig. 2. Results showed that zeolite could be identified as clinoptilolite and characteristic clinoptilolite peaks were recognized at $2\theta = 9.81°$, 22.3°, and 30°. Quartz peak at $2\theta = 26.62°$ was also identified. In literature, HCl treatment was reported to decrease the intensities of the characteristic peaks of zeolites [29]. However, results showed that characteristic peak intensities of the clinoptilolite were almost same compared to the control sample after the gastric treatment. It implied that crystal structure of zeolites were stable after gastric treatment where similar results were also reported [30]. On contrary, a significant change was observed in the quartz. HCl was a registered chemical used to purify the quartz [31]. It might help the diffusion of mineral impurities to the quartz crystal surface where they formed salts with chloride ion. Therefore, increase in peak intensity of the quartz might be related to the purification effect of HCl. At the later stages of the simulated digestion, with the increase in pH and with the complexation of the media, this purification was probably limited.

FTIR analyze for the gastric and intestinal digested zeolite samples were performed to investigate structural changes arised due to the simulated digestion treatments and results are given in Fig. 3. The 472 and 615 cm^{-1} peaks were assigned to the internal and external Si (or Al)–O double ring respectively. The strong symmetric and asymmetric stretch vibrations were present at 1,058 cm^{-1}. The water vibrations of zeolite were also observed after 3,450 cm^{-1}. In literature, acidic treatments were reported to result shifts at characteristic peaks position (at 472 and 1,056 cm^{-1}) and reduction in peak intensities were reported as a result of dealumination and partial structural breakdown [29, 32]. However, FTIR spectra showed that characteristic peaks of zeolite were preserved for all treatments and there were no significant variations in the frequencies of assigned bands after gastric and intestinal digestion processes. Therefore, there were no significant dealumination and structural breakdown and these results revealed that zeolites preserved their structural stability during simulated digestion.

FTIR results were also used to identify possibility of the adsorption of digestive media constituents onto zeolite surface. Results in Fig. 3 showed that there were no additional peaks in FTIR spectra of zeolites. Previous results of the interaction studies indicated that there were slightly changes in UV absorbance of the gastric media fluid (at 270 nm, corresponding to digestive enzymes) by zeolite treatment. However, this possible interaction especially between enzymes and zeolite should be so weak and it could not be observed in FTIR spectra.

To investigate possible interactions with the digestion media and the zeolite, IR spectrum of lyophilized powders of the digestion fluids were analyzed and results are given in Fig. 4. In Fig. 4, the main characteristic protein bands of digestive enzymes such as Amide 1 and Amide 3 are observed in the region around of 1,650 and 1,350 cm^{-1}. Possible hydrogen bonds to the C=O group were reported to lower the amide I frequency by 20–30 cm^{-1} and hydrogen bond to the NH group by 10–20 cm^{-1} [33]. However, no significant shifts were observed in digestion media powders with the zeolite treatments. Thus, result revealed that there was no hydrogen bonding and zeolite did't interact with C=O, C–N or N–H of the polypeptide chains in the digestive enzymes [34] which was also in

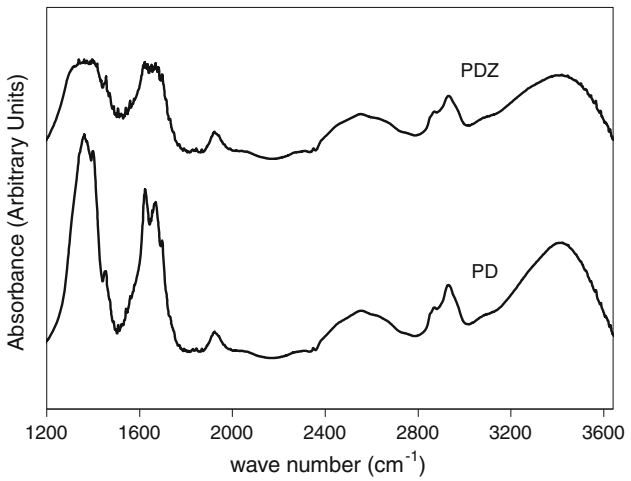

Fig. 4 Infrared spectra of simulated digestion fluid powders (*PD* powder of control digestion fluid, *PDZ* powder of digestion fluid incubated with zeolite)

Table 1 Elementary compositions of zeolite samples

Elements (mg g^{-1})	Zeolites		
	Z	ZG	ZD
Na	11.0 ± 2.3[a]	12.9 ± 3.0	19.7 ± 2.7
Mg	6.5 ± 2.0	6.1 ± 1.4	6.4 ± 1.7
Al	84.7 ± 5.0	81.5 ± 2.5	81.8 ± 8.4
Si	373.8 ± 12.6	368.8 ± 4.2	366.9 ± 1.5
K	24.2 ± 5.2	19.5 ± 0.7	18.4 ± 3.5
Ca	13.2 ± 3.7	13.5 ± 2.2	17.0 ± 4.0

Z untreated-control zeolite, *ZG* gastric treated zeolite, *ZD* digested zeolite

[a] SD of three replicates

good agreement with the FTIR results of the zeolite samples. Amide 2 bands (1,500–1,550 cm^{-1}) were not easily detected on the FTIR spectra because of the possible deformations with digestive treatment. This might be due to the proteolitic activity of digestive enzymes or changes in the pH and ionic strength of the media. Those factors might be effective in enzyme/protein stability and conformation. Additionally with digestion process using zeolite, intensities of the protein peaks were reduced. Similar results were also observed in UV spectrum of some liquid media samples as slight reduction in their intensities. Those reductions in the peak intensities might be due to the weak interactions of the digestion media components with zeolite.

With the pH change (from pH 2–7.5), there could be interactions between zeolite and digestive media and chemical composition of the zeolite might be affected. These interactions might be attributed to different physicochemical reactions as dissolution, ion exchange, sorption, and possibly surface precipitation [35]. Changes in the major elementary composition of zeolites were analyzed and results are given in Table 1.

Interactions of the zeolite with the digestive media might depend on Si/Al ratio and also could be related to acidic and basic sites in its structure which is defined by the Brønsted and Lewis theory. Such as, Si–O–Al species represents negative charge of the lattice and structural basic site. Therefore oxygen from the lattice acts as a proton acceptor. In simulated digestion experiments, pH adjustments were performed with $CaCO_3$ and NaOH so that they were in high amounts in the digestive media. Elementary composition results showed that Na^+ content of zeolite was increased especially after intestinal digestion experiments (79.1 %) which might be attributed to the exchange of this ion. It was important to note that Al composition was almost remained constant, however there were slight decrease in the Si composition with the increase in the pH of the digestive media. Such as, there was 1.3 and 1.8 % decrease in Si content compared to untreated-control zeolite (Z) after gastric and intestinal treatments, respectively. This might be related to the possible dissolution process of aluminosilicates at the surface layer at the alkaline conditions. The dissolution process for the natural zeolites were affected by the H^+ or OH^- in the solutions (Brønsted and Lewis theory) and they represent acidic or basic behavior. It was reported that dissolution of Si was related to the decrease in ionic strength and increase in the pH of the solution. Additionally Al dissolution was reported to be increased with the increase in ionic strength but also it decreased with the decrease in solution pH [26]. Therefore ionic strength and pH might be effective on slight dissolution of Si. However, Si content did not differ statistically from each other ($p < 0.05$) and dissolution might be considered as insignificant.

SEM images were recorded for the gastric and intestinal digested zeolite samples and results are given in Fig. 5. Results showed that hexagonal clinoptilolite crystals were identified in wide range of the samples. In simulated digestion treatment with the changes in pH, zeolites were subjected to acid or alkali media. Acidic and alkali conditions were reported to be effective in structural losses for zeolites which were defined by SEM analyzes [36, 37]. However, SEM results indicated that there was no structural deformation. Besides, no protein like structure was observed on the zeolite surface during scanning which was also in good agreement with the FTIR results.

SEM images were recorded for the lyophilized digestion media powders and results of 5,000× magnification were given in Fig. 6. Surface porosity and irregularity was observed but there wasn't a significant factor or relevance to differentiate the treatment types. On the other hand, it was interesting to observe that digested powders

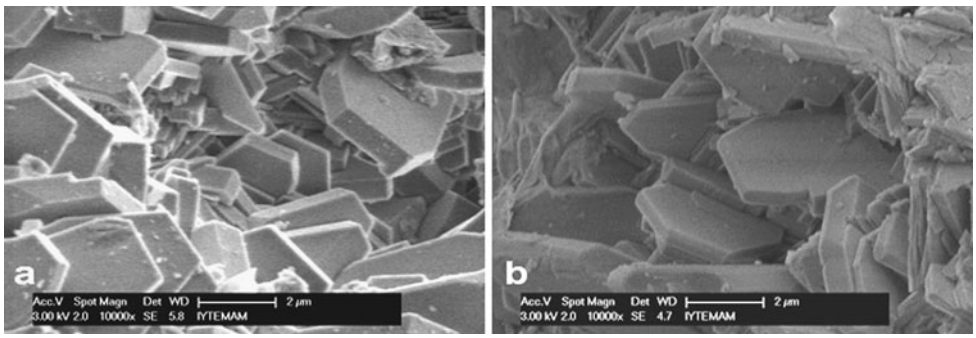

Fig. 5 SEM images of zeolites. **a** control-untreated zeolite (Z); **b** digested zeolite (ZD)

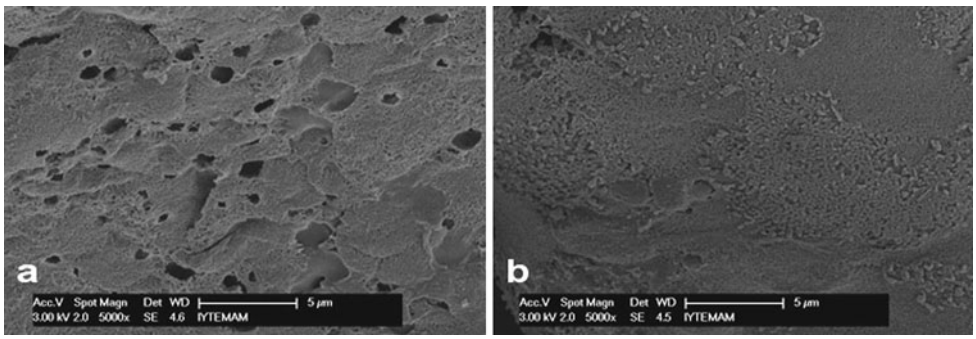

Fig. 6 SEM images of digestion fluid powders with ×5,000 magnification. **a** Powder of control digestion fluid (PD); **b** powder of digestion fluid incubated with zeolite (PDZ)

(without zeolite) were smaller in size but presence of the zeolite in the digestive media resulted powders to form aggregates (Fig. 7). Agglomeration is a sign of the existence of possible and complex interactions between the protein structures (enzymes) in the aqueous phase due to zeolite treatments. Proteins are often stable against aggregation over narrow pH ranges and when pH is outside those ranges, they may aggregate rapidly in solutions [38]. In simulated digestion process, digestion media contained the factors to prone aggregation of protein structures such as varying pH values and ionic strengths. Changes in pH (step by step; acidic to alkaline) and ionic strength of the media might have caused exchange of H^+ ions, binding of protons on the Lewis basic sites, removal of protons from the surface Bronsted acidic sites or removal of the protons that arrange the ion exchange (such as Na, K, Ca, Mg) [35] on zeolites surfaces. Although the exact mechanism was hard to define, this complex mechanism with zeolite treatments might have resulted proteins to possess anisotropic charge distribution on their surfaces and this might have caused increase in dipoles. Thus protein–protein interactions might be attractive and lead aggregation to be energetically favorable [39, 40].

3.3 Cytotoxicity results for Caco-2 cells

Caco-2 cells are originated from human digestive system that having primary importance for biomedical/drug applications. Possible metabolic events after zeolite exposure might lead to apoptosis or necrosis, and reduction in the cell viability of those cells. To investigate the effect of simulated digested clinoptilolite rich mineral on proliferation of human colon adenocarcinoma cells (Caco-2), cytotoxicity measurements were performed. Results were given in Figs. 8 and 9.

Results showed that both digested (ZD) and non-digested control zeolite (Z) were effective against cancer cell proliferations. Proliferation percentages varied in the range of 96.1–29.5 % with respect to zeolites, treatment time and zeolite concentration. Decrease in the cell viability might be related to the effect of zeolite on growth media. Because Caco-2 cells are enterocytes (absorbtive cells) and account for majority of the absorption in the small intestine [41] and they are highly sensitive to the changes in their microenvironment. Deviations from optimum conditions of Caco-2 cell growth in the culture media with zeolite treatments might have caused cells to go under stress and might have affected the Caco-2 cells responses. It was reported that the proton pumps in the Caco-2 cells did not rapidly reverse the effect of pH, and the buffering capacity of the cytoplasm was not strong enough to prevent the pH change [42]. Since zeolites have amphoteric behavior, they alter the pH of the aqueous growth media [30] thus reduction in cell proliferation compared to control sample might be achieved. Other possible reasons for the inhibition of cancer cell proliferation with zeolite treatment

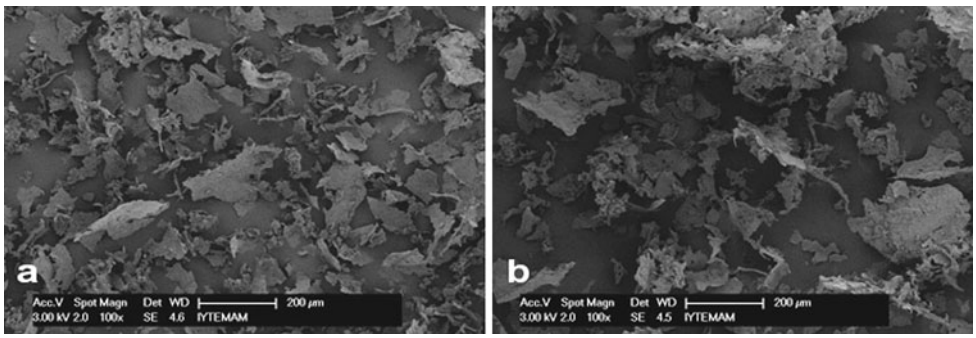

Fig. 7 SEM images of digestion fluid powders with ×100 magnification. **a** Powder of control digestion fluid (PD); **b** powder of digestion fluid incubated with zeolite (PDZ)

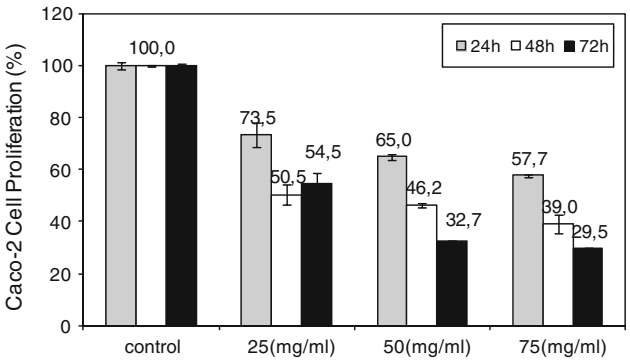

Fig. 8 Cell proliferation (%) for Caco-2 cells incubated with control zeolite (Z) treated culture media (incubation times: 24, 48 and 72 h; zeolite concentrations: 25, 50 and 75 mg/ml)

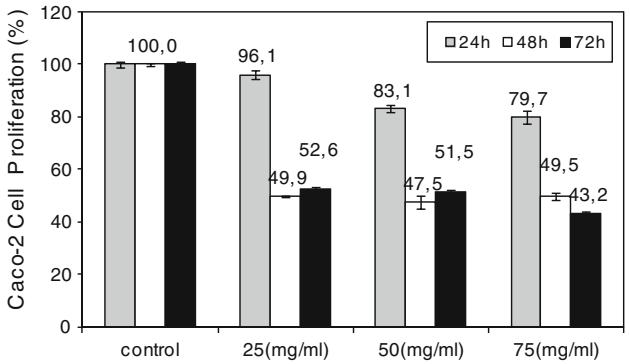

Fig. 9 Cell proliferation (%) for Caco-2 cells incubated with digested zeolite (ZD) treated culture media (incubation times: 24, 48 and 72 h; zeolite concentrations: 25, 50 and 75 mg/ml)

might due to its effect on cancer cell signaling pathways, or possibility of weak interactions such as van-der Waals, hydrogen bonding, electrostatic interactions between zeolite and some protein like structures in cell culture media (such as aminoacids, or growth hormones secreted by the cells) due to zeolite's ion exchange and adsorptive properties. Similar cases were suggested previously [21, 43]. It was reported that decrease in the viability of the tumor cells with the zeolite treatment might be due to adsorption of some serum components such as epidermal growth factor (EGF) by the clinoptilolite.

4 Conclusions

In this study, simulated digestion studies were performed in order to investigate the behavior clinoptilolite rich zeolites in in vitro simulated digestion conditions. Possible interactions of the clinoptilolite rich zeolites with digestive media and cytotoxic effects of their digested/non-digested forms on colon cancer cells (Caco-2) were analyzed. Overall results in this study indeed showed that the zeolites preserved their structural stability under given simulated digestion conditions. Additionally, cell culture studies indicated that clinoptilolite rich zeolite and its digested forms were both effective to inhibit colon cancer cell proliferation. Proliferation percentages reduced and varied in the range of 96.1–29.5 % with respect to zeolites, treatment time and zeolite concentration. However, agglomeration formation suggested the existence of possible and complex interactions among the protein structures (enzymes) in aqueous digestion media phase as a result of zeolite treatments. Considering potential biomedical applications of the clinoptilolite rich natural zeolites such as in drug systems or cancer therapy, this study is a primary step to understand possible interactions with complicated digestive media and their cytotoxicity against colon cancer cells. Further studies would be at the perspective of enzyme activity and cellular responses in molecular level regarding the pH and ionic strength which would be helpful to identify the detailed mechanism.

Acknowledgments This study was financially supported by Turkish Republic Prime Ministry State Planning Organization (DPT-2003K120690, Determination of Effects of Zeolite on Health at Cellular and Molecular Level). The authors gratefully acknowledge to Prof. Serdar ÖZÇELİK (Izmir Institute of Technology, Department of Chemistry, Turkey) for his kind contributions.

References

1. F. Mumpton, Proc. Natl. Acad. Sci. **96**, 3463 (1999)
2. A. Top, S. Ülkü, Appl. Clay Sci. **27**, 13 (2004)
3. B.C. Erdoğan, S. Ülkü, Micropor. Mesopor. Mat. **152**, 253 (2012)
4. D.S. Papaioannou, S.C. Kyriakis, A. Papasteriadis, N. Roumbies, A. Yannakopoulos, C. Alexopoulos, Res. Vet. Sci. **72**, 51 (2002)

5. M. Ortatatlı, H. Oğuz, Res. Vet. Sci. **71**, 59 (2001)
6. D.S. Papaioannou, C.S. Kyriakis, C. Alexopoulos, E.D. Tzika, Z.S. Polizopoulou, S.C. Kyriakis, Res. Vet. Sci. **76**, 19 (2004)
7. I. Martin-Kleiner, Z. Flegar-Mestric, R. Zadro, D. Breljak, S. Stanovic Janda, R. Stojkovic, M. Marusic, M. Radacic, M. Boranic, Food Chem. Toxicol. **39**, 717 (2001)
8. D. Prvulovic, A. Jovanovic-Galovic, B. Stanic, M. Popovic, G. Grubor-Lajsic, Czech J. Anim. Sci. **52**(6), 159 (2007)
9. M.D. Olver, Brit. Poultry Sci. **38**, 220 (1997)
10. S. Leung, S. Barrington, Y. Wan, X. Zhao, B. El-Husseini, Bioresour. Technol. **98**, 3309 (2007)
11. M.A Norouzian, R. Valizadeh, A. A. Khadem, A. Afzalzadeh, A. Nabipour, Biol. Trace Elem. Res. **137**, 168 (2010)
12. M. Ortatatli, H. Oguz, F. Hatipoglu, M. Karaman, Res. Vet. Sci. **78**, 61 (2005)
13. H. Oguz, Eurasian J. Vet. Sci. **27**(1), 1 (2011)
14. M. Topashka-Ancheva, M. Beltcheva, R. Metcheva, J.A. Rojas, A.O. Rodriguez-De la Fuente, T. Gerasimova, L. E. Rodríguez-Flores, S. E. Teodorova, Biol. Trace Elem. Res. (2011)
15. B. Mitrovic, G. Vitorovic, D. Vitorovic, A. Dakovic, M. Stojanovic, J. Environ. Radioactiv. **95**, 171 (2007)
16. K. Saribeyoglu, E. Aytac, S. Pekmezci, S. Saygili, H. Uzun, G. Ozbay, S. Aydin, H.O. Seymen, Asian J. Surg. **34**, 153 (2011)
17. A. Rivera, G. Rodrigiez-Fuentes, E. Altshuler, Micropor. Mesopor. Mat. **40**, 173 (2000)
18. G. Rodriguez-Fuentes, M.A. Barrios, A. Iraizoz, I. Perdoma, B. Cedre, Zeolites **19**, 441 (1997)
19. A. Rivera, G. Rodrigiez-Fuentes, E. Altshuler, Micropor. Mesopor. Mat. **24**, 51 (1998)
20. G. Rodriguez-Fuentes, A.R. Denis, M.A.B. Alvarez, A.I. Colarte, Micropor. Mesopor. Mat. **94**, 200 (2006)
21. K. Pavelic, M. Hadzija, L. Bedrica, J. Pavelic, I. Dikic, M. Katic, M. Kralj, M.H. Bosnar, S. Kapitanovic, M. Poljak-Blazi, S. Krizanac, R. Stojkovic, M. Jurin, B. Subotic, M. Colic, J. Mol. Med. **78**, 708 (2001)
22. A. Rivera, T. Farrias, A.R. Ruiz-Salvador, L.C. Menorval, Micropor. Mesopor. Mat. **61**, 249 (2003)
23. F. Esenli, Natural zeolite reserves, mining, production, and market situation. (National Zeolite Symposium, Tubitak-Mam, Gebze, Turkey, online published in Turkish). http://www.mam.gov.tr. Accessed 2 July 2002
24. Y. Akdeniz, S. Ülkü, J. Porous Mater. **14**, 55 (2007)
25. M.G. Ferruzzi, M.L. Failla, S.J. Schwartz, J. Agric. Food Chem. **49**, 2082 (2001)
26. M. Doula, A. Ioannou, A. Dimirkou, J. Colloid. Interf. Sci. **245**, 237 (2002)
27. D. Spelzini, J. Peleteiro, G. Picó, B. Farruggia, Colloid. Surface. B **67**, 151 (2008)
28. Q. Kang, X. Wu, Y. Xue, X. Liu, D. Shen, Sensor. Actuat. B-Chem. **61**, 68 (1999)
29. A. Arcoya, J.A. Gonzalez, N. Travieso, X.L. Seoane, Clay Miner. **29**, 123 (1994)
30. I. Polatoglu, F. Çakicioglu-Ozkan, Micropor. Mesopor. Mat. **132**, 219 (2010)
31. K.B. Loritsch, R.D. James, United States Patent No: 5,037,625 (1991)
32. F. Çakicioglu-Ozkan, S. Ülkü, Micropor. Mesopor. Mat. **77**, 47 (2005)
33. A. Barth, Biochim. Biophys. Acta **1767**, 1073 (2007)
34. S. Barral, M.A. Villa-García, M. Rendueles, M. Diaza, Acta Mater. **56**, 2784 (2008)
35. M. Trgo, J. Peric, J. Colloid Interf Sci. **260**, 166 (2003)
36. M. Ogura, S. Shinomiya, J. Tateno, Y. Nara, M. Nomura, E. Kikuchi, M. Matsukata, Appl. Catal. A-Gen. **219**, 33 (2001)
37. R. Rachwalik, Z. Olejniczak, B. Sulikowski, Catal. Today **114**, 211 (2006)
38. E.Y. Chi, S. Krishnan, T.W. Randolph, J.F. Carpenter, Pharmaceut. Res. **9**(20), 1325 (2003)
39. E.Y. Chi, S. Krishnan, B.S. Kendrick, B.S. Chang, J.F. Carpenter, T.W. Randolph, Protein Sci. **12**, 903 (2003)
40. A. Striolo, D. Bratko, J.Z. Wu, N. Elvassore, H.W. Blanch, J.M. Prausnitz, J. Chem. Phys. **117**(17), 7733 (2002)
41. P. Shah, V. Jogani, T. Bagchi, A. Misra, Biotechnol. Progr. **22**, 186 (2006)
42. E. Liang, P. Liu, S. Dinh, Int. J. Pharm. **338**, 104 (2007)
43. M. Katic, B. Bosnjak, K. Gall-Troselj, I. Dikic, K. Pavelic, Front Biosci. **11**, 1722 (2006)